

# Mesoporous TS-1 Nanocrystals as Low Cost and High Performance Catalysts for Epoxidation of Styrene

Tian-Lu Cui, Xin-Hao Li,\* and Jie-Sheng Chen\*

*School of Chemistry and Chemical Engineering, Shanghai Jiao Tong University, Shanghai 200240 China*

Mesoporous TS-1 nanocrystals were facilely synthesized without involving additional templates. The usage of inorganic silicon source, less structure-directing agent and high yields of nearly 100% made this template-free strategy suitable for large-scale synthesis with low cost. Furthermore, the as synthesized TS-1 exhibited comparable epoxidation performance than those obtained by other methods.

**Keywords** TS-1, mesoporous, nanocrystal, low cost, epoxidation

## Introduction

As an important class of crystalline metasilicates, titanium silicate-1 (TS-1) with uniform and ordered networks of micropores has been studied extensively with regards to various catalysts.<sup>[1]</sup> In particular, epoxidation of propylene, hydroxylation of phenol and ammoximation of cyclohexanone catalytic oxidation reactions using TS-1 and H<sub>2</sub>O<sub>2</sub> have been widely carried out in industry for the production of epoxypropane, dihydroxybenzene and cyclohexanone oxime.<sup>[1a,1b,2]</sup> TS-1 catalysts with low cost and high activity are highly desirable. It has been demonstrated that high catalytic activity can be obtained with TS-1 particle size smaller than 300 nm. Unfortunately, synthesis of small particle size TS-1 often needs organic silicon source such as tetraethylorthosilicate (TEOS) and a large amount of tetrapropylammonium hydroxide (TPAOH, structure-directing agent, SDA), both of which are extremely expensive.<sup>[3]</sup> Besides, the cost of separation was highly increased due to the small particle size. The high cost and unsatisfied catalytic performance of TS-1 catalysts drive materials scientists to redesign the mesoscale structure by using cheaper precursors.

Inexpensive silicon sources such as amorphous silica and low cost SDA like tetrapropylammonium bromide (TPABr) were utilized to partly or totally replace the expensive raw materials of TEOS and TPAOH.<sup>[3c,3d,4]</sup> Seeds-assistance method was also employed to synthesize small particle sized TS-1 with less amount of expensive organic ligands and silicon sources.<sup>[5]</sup> Besides, monolithic TS-1 materials were synthesized to reduce the cost of separation.<sup>[6]</sup> The dry-gel conversion and solvent-free method were also employed to synthesize

zeolites with high yield.<sup>[7]</sup> Meanwhile, many researches were carried out to improve the catalytic activity especially in the diffusion aspect by employing soft or hard template and fabricating other Ti-containing mesoporous zeolites.<sup>[8]</sup> However, seeds methods are either multistep or of low activity; mesoporous and monolithic materials often need various templates thus being high cost; other zeolites such as Ti-MCM-41 show lower activity due to the different titanium coordination environment.<sup>[9]</sup> More importantly, none of them can solve all problems in one-pot.

Herein, modified Kirkendall method which had been reported in our previous work was utilized to synthesize mesoporous TS-1 nanocrystals with the assistance of a little water by using inorganic silicon source (silica gel).<sup>[10]</sup> High concentration of TPAOH can be achieved by using less TPAOH (SiO<sub>2</sub>/TPAOH=8) due to the quasi-solid-state system. The separating procedure can also be omitted. Moreover, the as synthesized mesoporous TS-1 nanocrystals exhibited comparable epoxidation performance than those obtained by other methods.

## Experimental

### Synthesis of mesoporous TS-1 nanocrystals

Ti(OCH<sub>2</sub>CH<sub>2</sub>CH<sub>2</sub>CH<sub>3</sub>)<sub>4</sub> (TBOT) was mixed with silica gel (40 wt% in H<sub>2</sub>O) and TPAOH (25 wt% in H<sub>2</sub>O) with the molar ratio of the composition to be 100SiO<sub>2</sub> : 12.5TPAOH : 1TiO<sub>2</sub>. After the removal of water, the as-obtained dry gel (2 g) was mixed with 0.2 mL of water and then transferred to a Teflon-lined autoclave for further crystallization at 120 °C for 8 h. The as synthesized sample was dried and then heated at 550 °C in air for 6 h to remove organic components.

\* E-mail: xinhaoli@sjtu.edu.cn, chemcej@sjtu.edu.cn

Received October 24, 2016; accepted December 3, 2016; published online XXXX, 2017.

Supporting information for this article is available on the WWW under <http://dx.doi.org/10.1002/cjoc.201600701> or from the author.

In Memory of Professor Enze Min.

## Results and Discussion

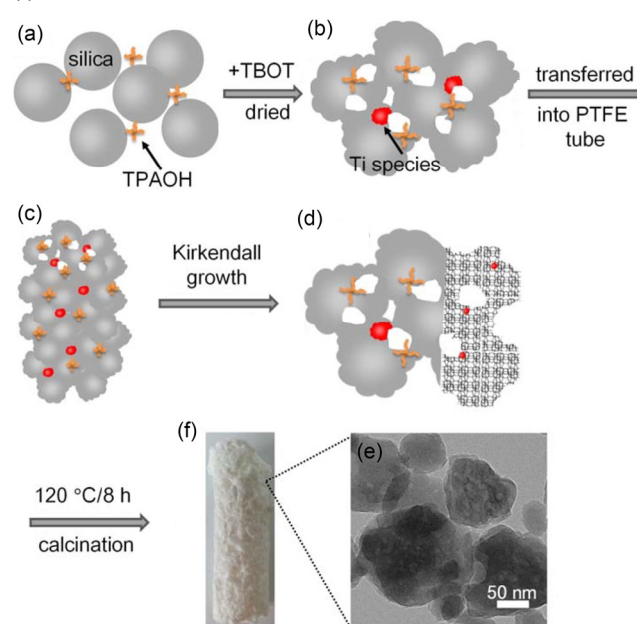
The overall growth process of mesoporous TS-1 nanocrystals was depicted in Scheme 1. Commercial silica nanoparticles were mixed with TPAOH with the molar ratio of 8SiO<sub>2</sub>/TPAOH and then the mixture (Scheme 1a) was mixed with TBOT under stirring. The homogeneous gel was dried at 60–70 °C to remove water and dried intermediates were gotten (Scheme 1b). During this process, intermediates were partially etched by TPAOH for further crystallization. The obtained mesoporous intermediates (dry gel) were transferred into a polytetrafluoroethylene tube (Scheme 1c) for further crystallization at 120 °C with assistance of limited amount of water. With the crystallization proceeding, the Kirkendall growth was triggered through chemical etching of dry gel by TPAOH and water. With the gradual diffusion of water vapor from outside of the precursors to the inside, crystallization of TS-1 proceeded accordingly. Nanovoids simultaneously diffused into TS-1, generating mesopores in situ as described in our previous work.<sup>[10]</sup> Besides, in this quasi-solid-state system the concentration of TPAOH could be as high as 15 mol·L<sup>-1</sup> even though the molar ratio of TPAOH/SiO<sub>2</sub> was as small as 1/8 (much lower than 3/7 of conventional method as shown in Table 1). In another word, TPAOH molecules were used in a more efficient manner here without a need of expensive and more complex organic surfactants, reducing the production cost effectively. On the other hand, the high concentration of TPAOH could help to form more nuclei and thus small size particles (Scheme 1e) even using inorganic silicon source. Furthermore, the simplified process without centrifuging (columnar sample could be obtained as shown in Scheme 1f) or filtration procedure can give high yields of mesoporous TS-1 nanocrystals more than 99%, much higher than that of samples obtained by the conventional method. It should be noted that the crystallization time was shortened to 8 h even under a lower reaction temperature of 120 °C. All these advantages made this strategy suitable for large scale production, especially from the perspective of the environment and economic issue. Detailed synthesis conditions of this template-free method as well as the conventional method were listed in Table 1.

Further textural characterizations were conducted to survey the property synthesized by this template-free

**Table 1** Synthesis conditions of samples obtained by different methods

	Conventional method	Our method
Silicon source	TEOS	silica gel
TPAOH/SiO <sub>2</sub>	3/7	1/8
Temperature/°C	170	120
Time/h	72	8
Yield/%	30–80	>99

**Scheme 1** The proposed synthesis processes of mesoporous TS-1 nanocrystals (a–d), the over-view transmission electron microscopy (TEM) image (e) and photo of the obtained sample (f)



strategy. As shown in Figure 1a, the X-ray diffraction patterns (XRD) of the typical sample demonstrated its high crystallinity with characteristic peaks of MFI structure. No other peaks assigned to titanium oxide could be detected indicating that the pure phase of the sample. Further diffuse reflectance UV-vis spectrum was carried out to determine the coordination environment of titanium. As shown in Figure 1b, the as synthesized sample showed a strong band centered at 205–215 nm, characteristic of tetrahedrally coordinated Ti species. Besides, it could be clearly observed that there was no obvious absorption band in the range of 300–350 nm, excluding the formation of TiO<sub>2</sub> particles.<sup>[11]</sup> Thus, it can be concluded that all the Ti atoms enter the framework. The molar ratio of Ti/Si was estimated to be 1/98 according to the X-ray fluorescence spectrometer (XRF) analysis, in agreement with that of the raw (1/100). The scanning electron microscope (SEM) image and the corresponding elemental mapping image (Figure S1) further indicated the homogeneous distribution of Ti species in the synthesized TS-1 sample.

The high resolution SEM image shown in Figure 2a revealed the small size of the sample with a mean size around 130 nm, matching well with the over-view transmission electron microscopy (TEM) image of Scheme 1e and demonstrated that nanosized TS-1 could be obtained even without the involvement of organic silicon source as well as large amounts of TPAOH. Figure 2b showed the high resolution TEM (HRTEM) image of nanosized TS-1. The clearly distinguishable lattice fringes revealed the high crystallinity of the whole nanoparticle which was also reflected by the XRD pat-

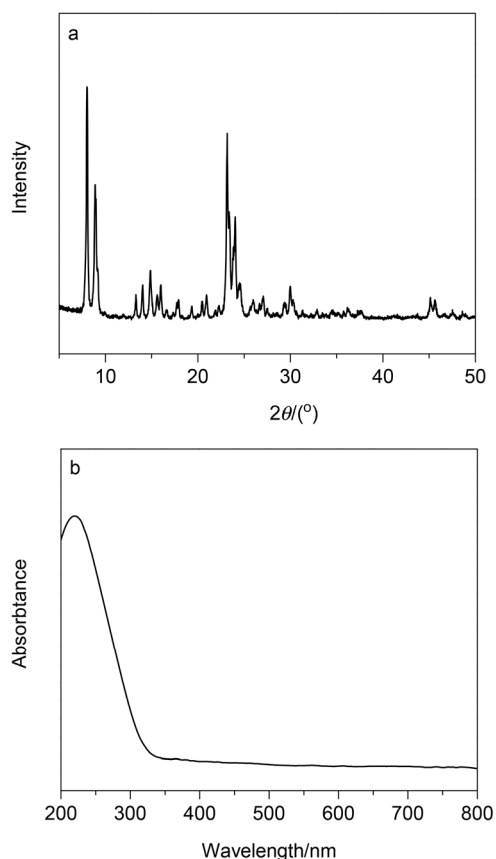


**Figure 1** (a) XRD pattern and (b) diffuse reflectance UV-visible spectrum of the as synthesized sample.

terns as show in Figure 1a. It could also be observed that there existed brighter areas in the TEM image and the observation was more clearly in the large scale TEM image of Scheme 1e, suggesting the formation of mesopores distributing homogeneously in each nanoparticles. The mesoporous properties of the as synthesized TS-1 nanoparticles could also be reflected by the  $N_2$  adsorption/desorption isotherms and the corresponding pore size distribution as shown in Figures 1c and 1d. The  $N_2$  adsorption/desorption isotherms (Figure 1c) exhibit a steep uptake at the low relative pressure which signifies the presence of microporosity in the TS-1 nanoparticles, being agree with the XRD and HRTEM results as shown in Figures 1a and 2b. Furthermore, the isotherms exhibit two hysteresis loops at relative pressure  $p/p_0$  of 0.20–0.40 and 0.85–1.00, indicating the formation of bimodal mesopores in the sample. These results were also consistent with the TEM observation (Scheme 1e and Figure 2b) and could be clearly reflected by the Barret-Joyner-Halenda pore size distribution as shown in Figure 2d. Moreover, the as synthesized mesoporous TS-1 nanocrystals showed high total as well as mesopore volume of 0.46 cc/g and 0.34 cc/g, respectively (Table S1).

In order to confirm the advantages of mesoporous TS-1 nanocrystals, much effort has also been directed towards catalytic performance.<sup>[12]</sup> Epoxidation of styrene was selected as a model reaction, which is of par-

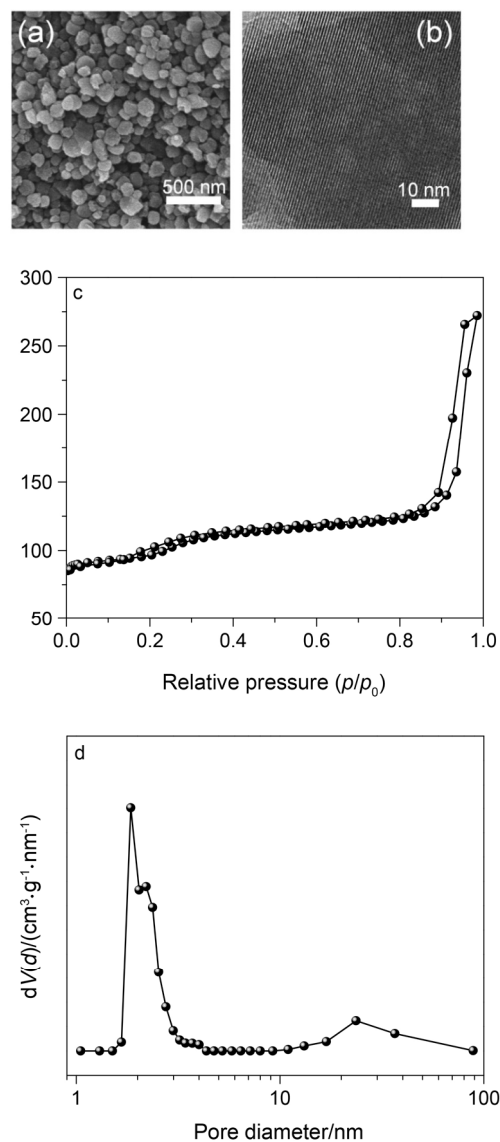


**Figure 2** (a) SEM image, (b) HRTEM image, (c)  $N_2$  adsorption-desorption isotherm and (d) BJH pore size distribution of the as synthesized sample.

ticular interest from both scientific and commercial point of view. As shown in Figure 3, both mesoporous TS-1 nanocrystals (meso-TS-1) and the control sample (bulk-TS-1) gave the same products of styrene oxide, benzaldehyde and phenylacetaldehyde. The selectivity of each product was similar while the conversions were various. As expected, meso-TS-1 offered much higher conversions as compared with the corresponding bulk phases (bulk-TS-1). Meso-TS-1 sample offered a much higher conversion of 51.7 %, almost two times of that of bulk-TS-1 (26.7%). It should be noted that the Ti content of meso-TS-1 was lower than that of bulk-TS-1 as shown in Table S1. The turn over frequency (TOF) values for oxidation of styrene over meso-TS-1 and bulk-TS-1 were also estimated to better reflect the catalytic performance of the two samples. As shown in Table S1, meso-TS-1 offered a TOF value of 71.7 mol (styrene)  $\text{mol}^{-1}$  metal  $\text{h}^{-1}$ , while that of bulk-TS-1 was

only 28.2 mol styrene mol<sup>-1</sup> metal h<sup>-1</sup>. Obviously, it is the unique mesoporous nanostructure of TS-1 with shortened mass transfer path that promoted their catalytic activity. Moreover, the TOF values of meso-TS-1 surpassed those of typical TS-1 and other MFI based catalysts for the same reaction in the literature (Table S2). All these results promise great potentials of mesoporous TS-1 nanocrystals as efficient catalysts.

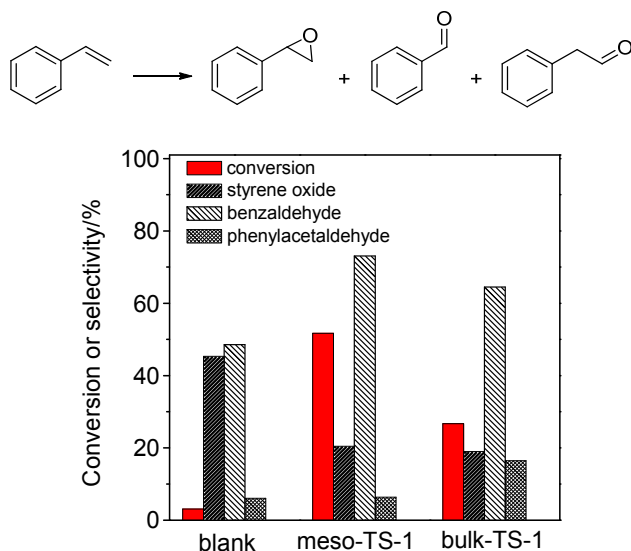


**Figure 3** Catalytic performance of styrene epoxidation over various samples. Typical reaction conditions for epoxidation of styrene: 5 mmol styrene, 50 mg of catalyst, 10 mmol H<sub>2</sub>O<sub>2</sub> (30% aqueous), 2.5 mL of CH<sub>3</sub>CN, 70 °C, 4 h. The mesoporous TS-1 nanocrystals were denoted as meso-TS-1, whilst corresponding bulk phases (bulk-TS-1) was also tested as control sample.

## Conclusions

In summary, we have successfully synthesized mesoporous TS-1 zeolites through the Kirkendall effect on the growth of zeolite nanocrystals. Inorganic silicon source, lower consumption of organic base TPAOH, high yields, mild synthetic conditions, high mesoporosity and small particle size, all these features make our template-free method suitable for large-scale synthesis of functional nanocrystals of mesoporous zeolites with relatively low cost for practical uses. The advantages of mesoporous-microporous zeolites have already been demonstrated by the much better catalytic performance as compared with bulk phase counterparts. More efforts will be devoted to extending our method to the fabrication of other microporous zeolites (e.g. FAU, LTA, Beta, MOR) for specific purpose of their real applications in the future.

## Acknowledgement

This work was financially supported by National Basic Research Program of China (2013CB934102), the National Natural Science Foundation of China

(21331004, 21301116) and Shanghai Eastern Scholar Program.

## References

- [1] (a) Zhou, J.; Hua, Z.; Cui, X.; Ye, Z.; Cui, F.; Shi, J. *Chem. Commun.* **2010**, 46, 4994; (b) Zhang, X.; Wang, Y.; Xin, F. *Appl. Catal. A: Gen.* **2006**, 307, 222; (c) Na, K.; Jo, C.; Kim, J.; Ahn, W. S.; Ryoo, R. *ACS Catal.* **2011**, 1, 901; (d) Serrano, D.; Sanz, R.; Pizarro, P.; Moreno, I.; Medina, S. *Appl. Catal. B: Environ.* **2014**, 146, 35.
- [2] Lin, M.; Xia, C.; Zhu, B.; Li, H.; Shu, X. *Chem. Eng. J.* **2016**, 295, 370.
- [3] (a) Wilkenhöner, U.; Langhendries, G.; Laar, F.; Baron, G. V.; Gammon, D. W.; Jacobs, P. A.; Steen, E. *J. Catal.* **2001**, 203, 201; (b) Tuel, A.; Taarit, Y. B. *Appl. Catal. A: Gen.* **1993**, 102, 69; (c) Gontier, S.; Tuel, A. *Zeolites* **1996**, 16, 184; (d) Wang, X. S.; Guo, X. W. *Catal. Today* **1999**, 51, 177.
- [4] (a) Iwasaki, T.; Isaka, M.; Nakamura, H.; Yasuda, M.; Watano, S. *Microporous Mesoporous Mater.* **2012**, 150, 1; (b) Deng, X.; Wang, Y.; Shen, L.; Wu, H.; Liu, Y.; He, M. *Ind. Eng. Chem. Res.* **2013**, 52, 1190.
- [5] (a) Grieneisen, J.; Kessler, H.; Fache, E.; Le Govic, A. *Microporous Mesoporous Mater.* **2000**, 37, 379; (b) Xue, T.; Wang, Y. M.; He, M. *Microporous Mesoporous Mater.* **2012**, 156, 29.
- [6] Yang, L.; Xin, F.; Lin, J.; Zhuang, Z.; Sun, R. *RSC Adv.* **2014**, 4, 27259.
- [7] (a) Meng, X.; Wu, Q.; Chen, F.; Xiao, F. S. *Sci. China Chem.* **2015**, 58, 6; (b) Zhu, L.; Zhang, J.; Wang, L.; Wu, Q.; Bian, C.; Pan, S.; Meng, X.; Xiao, F. S. *J. Mater. Chem. A* **2015**, 3, 14093.
- [8] (a) Xin, H.; Zhao, J.; Xu, S.; Li, J.; Zhang, W.; Guo, X.; Hensen, E. J.; Yang, Q.; Li, C. *J. Phys. Chem. C* **2010**, 114, 6553; (b) Zhu, Y.; Hua, Z.; Zhou, X.; Song, Y.; Gong, Y.; Zhou, J.; Zhao, J.; Shi, J. *RSC Adv.* **2013**, 3, 4193; (c) Liang, W.; Jin, Y.; Yu, Z.; Wang, Z.; Han, B.; He, M.; Min, E. *Zeolites* **1996**, 17, 297; (d) Wu, P.; Nuntasri, D.; Ruan, J.; Liu, Y.; He, M.; Fan, W.; Terasaki, O.; Tatsumi, T. *J. Phys. Chem. B* **2004**, 108, 19126; (e) Sun, M.; Zhao, T.; Wang, J.; Ma, Z.; Li, F. *Chin. J. Chem.* **2015**, 33, 1057; (f) Koohsaryan, E.; Anbia, M. *Chin. J. Catal.* **2016**, 37, 447.
- [9] (a) Blasco, T.; Corma, A.; Navarro, M.; Pariente, J. P. *J. Catal.* **1995**, 156, 65; (b) Han, Y.; Xiao, F. S.; Wu, S.; Sun, Y.; Meng, X.; Li, D.; Lin, S.; Deng, F.; Ai, X. *J. Phys. Chem. B* **2001**, 105, 7963; (c) Clerici, M. G.; Domine, M. E. *Liquid Phase Oxidation via Heterogeneous Catalysis*, John Wiley & Sons, Inc. **2013**, p. 21; (d) Li, C.; Xiong, G.; Xin, Q.; Liu, J.; Ying, P.; Feng, Z.; Li, J.; Yang, W.; Wang, Y.; Wang, G.; Liu, X.; Lin, M.; Wang, X.; Min, E. *Angew. Chem., Int. Ed.* **1999**, 38, 2220.
- [10] (a) Cui, T. L.; Li, X. H.; Lv, L. B.; Wang, K. X.; Su, J.; Chen, J. S. *Chem. Commun.* **2015**, 51, 12563; (b) Cui, T. L.; Ke, W. Y.; Zhang, W. B.; Wang, H. H.; Li, X. H.; Chen, J. S. *Angew. Chem., Int. Ed.* **2016**, 55, 9178; (c) Cui, T. L.; Lv, L. B.; Zhang, W. B.; Li, X. H.; Chen, J. S. *Catal. Sci. Technol.* **2016**, 6, 5262.
- [11] Zecchina, A.; Spoto, G.; Bordiga, S.; Ferrero, A.; Petrini, G.; Leofanti, G.; Padovan, M. *Stud. Surf. Sci. Catal.* **1991**, 69, 251.
- [12] (a) Tian, Y.; Li, G. D.; Chen, J. S. *J. Am. Chem. Soc.* **2003**, 125, 66223; (b) Li, L.; Zhou, X. S.; Li, G. D.; Pan, X. L.; Chen, J. S. *Angew. Chem., Int. Ed.* **2009**, 48, 6678; (c) Li, L.; Li, G. D.; Yan, C.; Mu, X. Y.; Pan, X. L.; Zou, X. X.; Wang, K. X.; Chen, J. S. *Angew. Chem., Int. Ed.* **2011**, 50, 8288; (d) Li, L.; Cai, Y. Y.; Li, G. D.; Mu, X. Y.; Wang, K. X.; Chen, J. S. *Angew. Chem., Int. Ed.* **2012**, 51, 4702; (e) Li, X. H.; Baar, M.; Blechert, S.; Antonietti, M. *Sci. Rep.* **2013**, 3, 1743; (f) Li, X. H.; Cai, Y. Y.; Gong, L. H.; Fu, W.; Wang, K. X.; Bao, H. L.; Wei, X.; Chen, J. S. *Chem. Eur. J.* **2014**, 20, 16732; (g) Wang, J. F.; Wang, K. X.; Wang, J. Q.; Li, L.; Chen, J. S. *Chem. Commun.* **2012**, 48, 2325.

(Pan, B.; Fan, Y.)